

Nonlinear Finite Analysis of Structural Behavior of Brick Masonry-Infilled Reinforced Concrete Frames

Mahmud Kori Effendi¹, Astriana Hardawati^{2,*}, Siti Aliyyah Masjuki³

¹Department of Civil Engineering, Universitas Janabadra, Yogyakarta, INDONESIA

²Department of Civil Engineering, Universitas Islam Indonesia, Yogyakarta, INDONESIA

³Department Of Civil Engineering, International Islamic University Malaysia, Kuala Lumpur, MALAYSIA

*Corresponding author: harda.astriana@uii.ac.id

SUBMITTED 19 July 2024 REVISED 20 August 2024 ACCEPTED 14 February 2025

ABSTRACT Earthquake disasters are among the most significant causes of structural failure, often resulting in buildings either collapsing entirely or sustaining partial damage that renders them unusable. The construction of unreinforced brick walls has been a traditional practice in Indonesia since ancient times. In this present study, a simplified representation of earthquake loading is achieved by applying a lateral static load to the brick walls. The research investigates the influence of concrete frame strength on brick walls, using specimens made of good-quality concrete (wall configuration 1) and poor-quality concrete (wall configuration 2). Three-dimensional finite element analysis was conducted using MSC Marc/Mentat software to validate the numerical findings against experimental results. In the finite element model, the concrete frame is represented by 3D solid elements, while the reinforcing steel is modeled using 3D truss elements. The stress-strain relationship is defined as multilinear for concrete and bilinear for reinforcing steel. The modified Kent-Parker model is employed to characterize the multilinear stress-strain behavior of brick wall macro-elements. Additionally, linear Mohr-Coulomb plasticity and isotropic hardening flow plasticity are used to simulate the mechanical behavior of concrete and brick walls. Contact interactions between the concrete frame and walls are also incorporated into the analysis. The loading is applied in-plane using force-controlled conditions. The results of the analysis reveal that the deformation patterns of brick walls differ significantly between wall configuration 1 and wall configuration 2. These differences arise due to variations in the concrete strength of the frames, which influence the walls' deformation characteristics. Finite element analysis further indicates that the initial stiffness of the brick walls aligns well with experimental findings, with nonlinearity observed only in wall configuration 2. The total strain contour analysis shows that failure in wall configuration 1 occurs along a diagonal plane, while in wall configuration 2, the failure path is diagonal but exhibits an upward curvature.

KEYWORDS Brick; Wall; Macro element; Finite Element; In-Plane Loading

© The Author(s) 2025. This article is distributed under a Creative Commons Attribution-ShareAlike 4.0 International license.

1 INTRODUCTION

In Indonesia, earthquakes are a common natural disaster that often cause infrastructure to experience total collapse or partial damage, rendering it unusable. Generally, brick walls are widely used in houses, but they can be also employed in various types of buildings, such as industrial structures, religious facilities, and shopping malls (Abdessemed-Foufa, 2017; Bhatti et al., 2017; Johansson et al., 2019). These buildings likely utilize brick walls due to the material's inherent advantages. Some benefits of brick wall construction include weather resistance, fire protection, and insulation against heat and sound (Hendry and Khalaf, 2017). Masonry construction, particularly confined or unreinforced masonry, is extensively used for residential buildings in Indonesia. In Banda Aceh, Sumatra, many buildings incorporate brick masonry as fillers for walls damaged by earthquakes (Brzev and Mitra, 2007).

Apart from conducting experiments, numerical analysis serves as an effective tool for studying the behavior of masonry walls under lateral and/or gravity loads. The finite element method (FEM) is a robust numerical

analysis technique widely employed to solve complex engineering and physical problems described by partial differential equations. In the finite element analysis of masonry walls subjected to lateral and/or gravity loads, brick walls are typically modeled using one of the following approaches: (i) the macro-modeling approach (da Silva and Milani, 2022; Grzyb and Jasiński, 2022; Panto et al., 2019); (ii) the detailed micro-modeling approach (Gaetano et al., 2022; Naciri et al., 2021); and (iii) the simplified micro-modeling approach (Chen et al., 2023; Greco et al., 2020).

The selection of the type of element is important to accurately represent the brick wall structure, whether confined or unconfined by a concrete frame. Some researchers use plane stress elements (Weber et al., 2021; Chaker et al., 2022; Noor-E-Khuda et al., 2016; Triwiyono and Eratodi, 2019) and also use solid elements to model brick walls (Plassiard et al., 2021; Muhit et al., 2022; Ravichandran et al., 2021; Scacco et al., 2020).

A study on finite element analysis using the ADINA

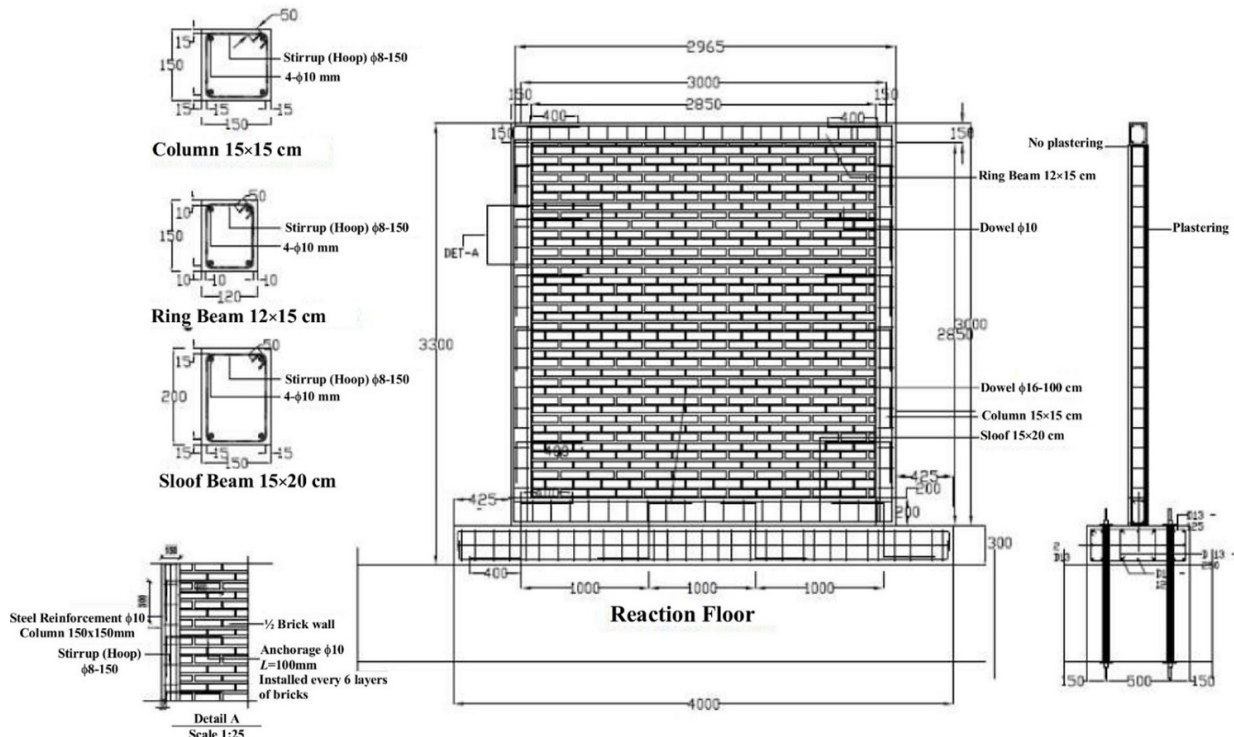


Figure 1 Experimental data verification of brick wall (Triwiyono and Eratodi, 2019)

Table 1. Wall configurations (Triwiyono et al., 2020)

Configuration Number	Brick	Concrete	Mortar
Wall configuration 1	Good	Good (1:2:3:0.8)	Good
Wall configuration 2	Good	Bad (1:2:3:1.2)	Good

Table 2. Mechanical properties of specimens (Triwiyono et al., 2020)

No	Testing	Results
1	Steel Tensile Test, $\phi 10$	
	f_y (MPa)	386.37
	f_u (MPa)	550.32
	E (MPa)	197,725
2	Steel Tensile Test, $\phi 8$	
	f_y (MPa)	405.56
	f_u (MPa)	506.86
	E (MPa)	197,725
3	Brick Masonry (Good)	
	Compression Strength, f_m (MPa)	3.25
	Tensile Strength (MPa)	0.21
	Modulus of Elasticity (MPa)	2,400
4	Concrete Test (Good)	
	Compression Strength (MPa)	19.08
	Modulus of Elasticity (MPa)	24,855.57
5	Concrete Test (Bad)	
	Compression Test (MPa)	15.48
	Modulus of Elasticity (MPa)	24,855.57

software for confined brick walls was conducted by Triwiyono and Eratodi (Triwiyono and Eratodi, 2019). This research utilized orthotropic elements to model the brick wall components. The results of the finite element analysis revealed a significant discrepancy in the initial stiffness values when compared to experimental observations. In the present research, finite element analysis using MSC Marc/Mentat software employs an isotropic material macro-modeling approach to model brick wall elements. Macro-modeling simplifies the analysis of brick masonry walls by representing them as a single, uniform material, enabling the evaluation of overall structural behavior without detailing each individual brick and mortar joint.

This study aims to evaluate the results of a newly developed finite element model by comparing them with experimental results for masonry walls confined within concrete frames. To verify the finite element results, research from Triwiyono (Triwiyono and Eratodi, 2019; Triwiyono et al., 2020) was used. In this study, three-dimensional finite element modeling of brick masonry walls with concrete frame constraints was conducted by implementing the MSC Marc/Mentat software (Öchsner and Öchsner, 2016). The parameters studied in this finite element analysis include the influence of the good-quality of clay bricks confined with both good-and-poor-quality of concrete frames. The finite element study uses a macro-element approach with contact analysis between the brick masonry wall and the concrete frame. The load applied to the brick wall structure is a lateral static load.

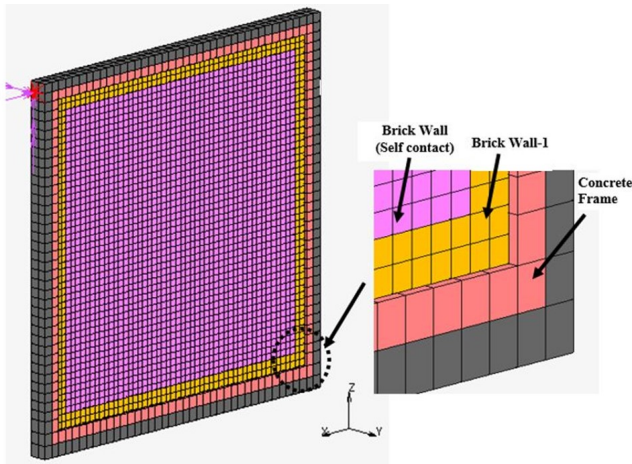


Figure 2 Contact analysis in the brick wall model

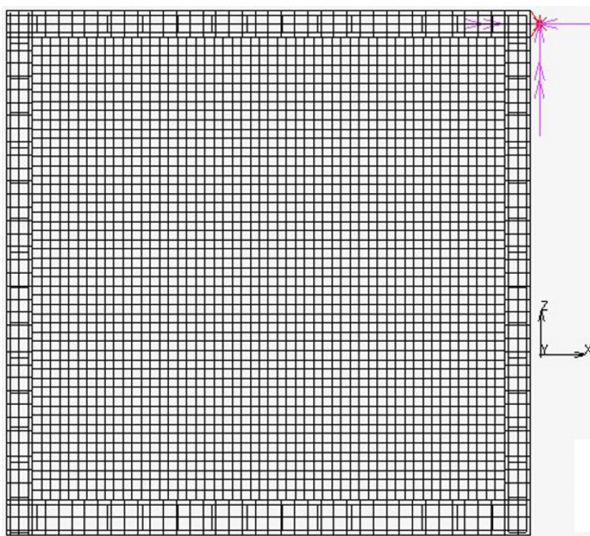


Figure 3 Meshing of the specimen

2 RESEARCH METHODOLOGY

2.1 Experimental Data for Verification

The experimental data by Triwiyono (Triwiyono and Eratodi, 2019) are used as validation for the finite element analysis. The experiment involves the brick masonry walls with dimensions of 3 × 3 m. This wall is confined on every side by beams and columns. The dimensions of the columns, ring beam, and sloop beam are 0.15 × 0.15 m, 0.12 × 0.15 m, and 0.15 × 0.2 m, respectively. The bricks were made from local clay with approximate dimensions of 22 cm in length, 10 cm in width, and 5.5 cm in thickness. The dimensions, reinforcement details of the reinforced concrete frame, brick wall, wall anchorage, and foundation anchorage are shown in Figure 1.

The results of this finite element analysis are validated against two experimental results from Triwiyono and Eratodi (Triwiyono and Eratodi, 2019). The configuration of these walls is presented in Table 1.

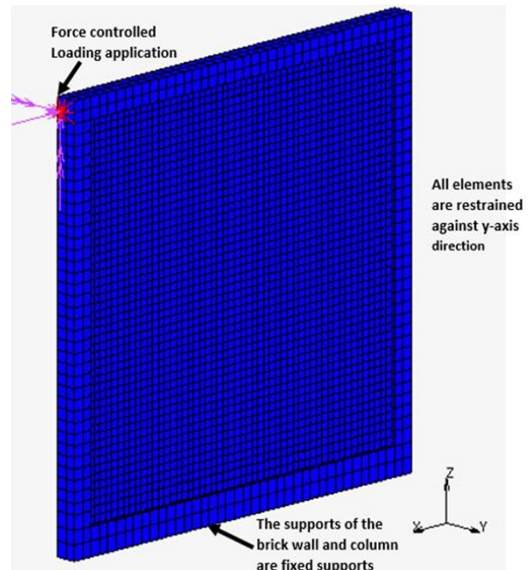


Figure 4 Loading condition, boundary condition, and supports

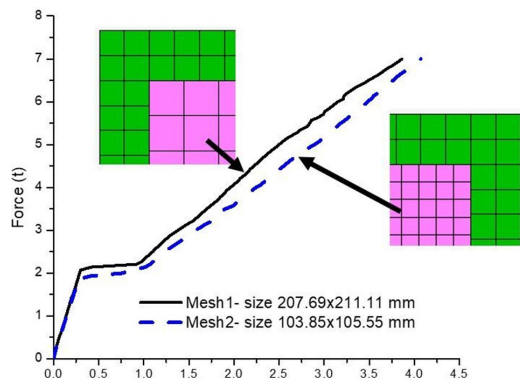


Figure 5 Force vs. displacement results for the different element sizes

These wall configurations represent brick walls with good and poor-quality materials. The material properties for steel reinforcement, stirrup, brick masonry and concrete, obtained from laboratory test, are given in Table 2. The compressive strength of the concrete was classified as either good or poor quality based on the proportions of aggregate, sand, cement, and the water-to-cement ratio. Specifically, the proportions were 3:2:1:0.8 and 3:2:1:1.2, respectively (Triwiyono and Eratodi, 2019). The quality of bricks was determined qualitatively based on the International Association for Earthquake Engineering (IAEE) guidelines (Arya et al., 2014).

2.2 Finite Element Analysis

The three-dimensional finite element analysis has been carried out with MSC Marc/Mentat 2012 software for modeling brick masonry wall. Using MSC Marc/Mentat for finite element analysis (FEA) offers distinct advantages, especially for complex, nonlinear problems (Marc, 2012a). The brick model is simpli-

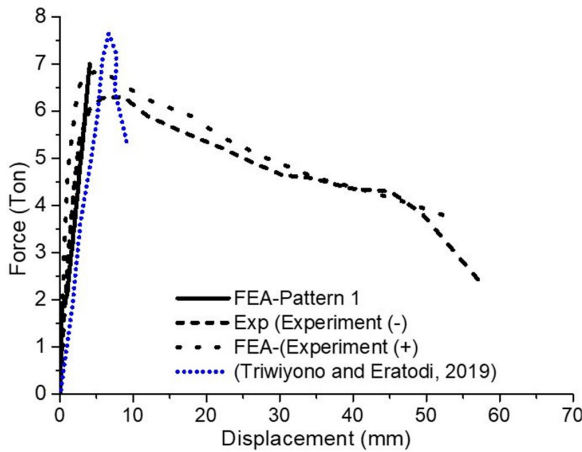


Figure 6 Force and displacement response-Configuration 1

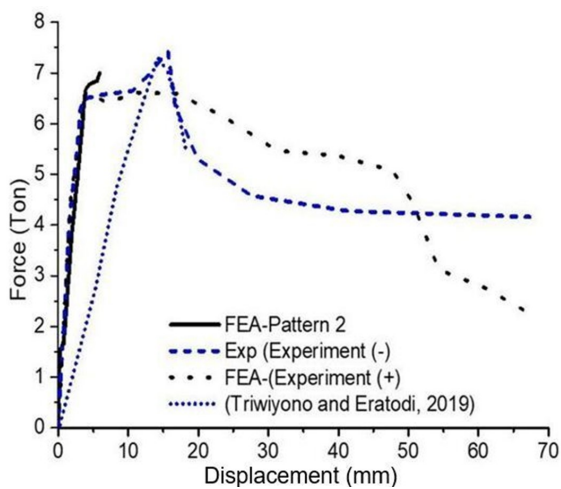


Figure 7 Force and displacement response-Configuration 2

fied using a macro-modeling approach in finite element analysis to represent the structural behavior of masonry walls.

2.2.1 Material model

The beam, column, and brick wall are represented by solid elements. The Linear Mohr-Coulomb plasticity model is used to simulate the brick masonry and concrete beams and columns under compression. Both the tensile stress in concrete and brick walls is assumed to be small to account for the fact that the tensile strength of concrete is generally considered negligible. The strain hardening follows the isotropic hardening rule (Marc, 2012a). The material properties of concrete and steel are adopted based on the findings of Triwiyono's study (Triwiyono et al., 2020). The remaining properties, including a specific gravity of $2,402.76 \text{ kgm}^{-3}$, a modulus of elasticity of $24,855.57 \text{ MPa}$, and a Poisson's ratio of 0.2, were assumed.

The stirrup and longitudinal steel are represented using 3D truss elements. The steel model is bilinear. The input parameters used for steel reinforcement material

are specific gravity = $7,850 \text{ kgm}^{-3}$, Modulus of Elasticity = $19,7724.7 \text{ MPa}$, and Poisson's ratio = 0.3. The von Mises yield criteria is used to describe the plasticity of the reinforcement. For strain hardening, the isotropic hardening rule is applied (Marc, 2012b).

Brick masonry modeling for structural analysis encompasses a range of methodologies. Among these, one approach involves modeling brick walls using macro-element techniques. The "modified" Kent-Park model adequately predicts the stress-strain relationship of clay brick masonry (Ewing and Kowalsky, 2004). The equation used is as follows:

for $0 \leq \varepsilon_m \leq 0.0015$ (parabolic rising curve)

$$f_m = 1.067 f_m \left[\frac{2\varepsilon_m}{0.002} - \left(\frac{\varepsilon_m}{0.002} \right)^2 \right] \quad (1)$$

For descending curve until $0.2f_m$

$$f_m = f_m [1 - Z_m (\varepsilon_m - 0.0015)] \quad (2)$$

where

$$Z_m = \frac{0.5}{\left[\frac{3+0.29f_j}{145f_j-1000} \right] - 0.002} \quad (3)$$

f_m and ε_m = compressive stress and strain in masonry, respectively f'_m = compressive prism strength of masonry f_j = compressive strength of mortar.

2.2.2 Contact analysis

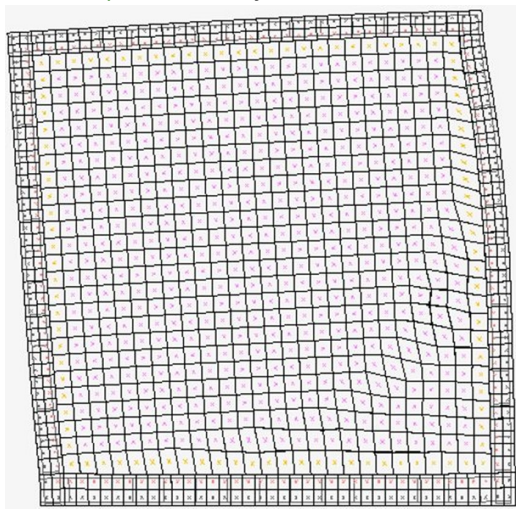
The contact between the concrete frame elements and the brick wall elements, which assumes that shared nodes exist between the brick elements and the concrete frame, has been used in research on confined brick walls by Triwiyono (Triwiyono et al., 2020). In this present study, contact analysis was carried out for finite element modeling using MSC Marc/Mentat software. In Figure 2, for brick wall elements, the contact between the elements that make up the brick wall (self-contact) is modeled. However, wall plastering mortar is not modeled in the finite element model, so that there is a gap between the frame elements and the brick wall elements. Brick wall-1 elements are in contact with the concrete frame. All contacts are modeled using the contact a type designated as glue. Glue contact in finite element analysis is employed to simplify the modeling of dowel anchors within the experimental framework. While the physical experiment demonstrated separation between the concrete frame and the brick wall, the dowel anchorage mechanism in the finite element model was idealized as a perfect bond. This assumption ensures no relative motion or separation occurs at either interfaces.



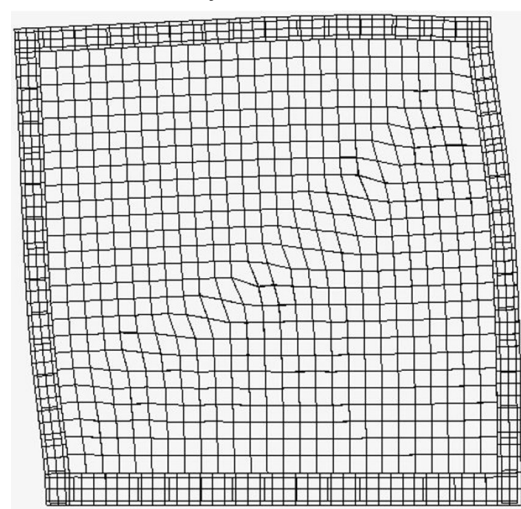
(a) Tie beam and foundation separation of experimental specimen (Triwiyono et al., 2020)



(b) Spalling at the bottom corner of the concrete frame (Triwiyono et al., 2020)



(c) Wall configuration 1 deformed shape of FEA analysis



(d) Wall configuration 2 deformed shape of FEA analysis

Figure 8 Deformed shape

2.2.3 Modeling of Finite Element

The mesh of the confined brick masonry wall can be seen in Figure 3. In this modeling, flexural reinforcement and shear reinforcement truss elements are embedded in beam and column solid elements. This method has been implemented in reinforced concrete beams by Effendi (Effendi, 2020).

The boundary and loading conditions can be seen in Figure 4. The in-plane loading is applied by the force control with a maximum value of 7 tons. The loading is implemented using multi-point-constraints with a rigid bar element. The support boundary conditions were specified as fixed degrees of freedom. All the elements of the brick masonry wall specimen in this modeling are constrained from moving along the Y axis.

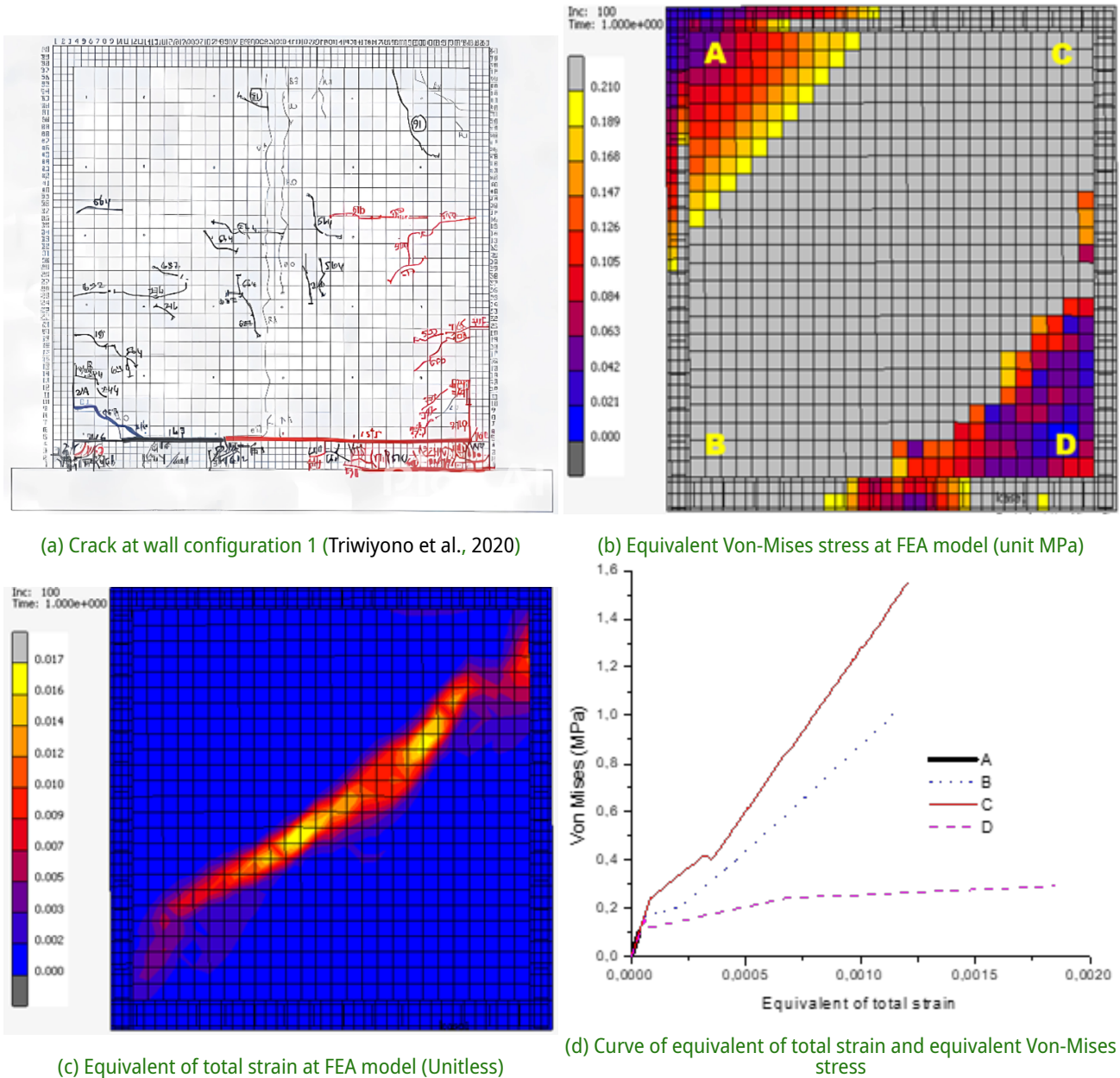
Mesh sensitivity analysis is performed to select the appropriate mesh size that provides accurate results with optimal computation time. In finite element modeling,

the plaster on the wall is not modeled, so that the concrete frame mesh width is 75 mm, and the wall mesh width is 52 mm. The brick wall mesh of $207.69 \times 211.11 \times 52$ mm (Mesh 1) and $103.85 \times 105.55 \times 52$ mm (Mesh 2) are used in the mesh sensitivity analysis. The force-displacement plotting results can be seen in Figure 5. The Mesh 2 model was considered during the analysis.

3 RESULTS AND DISCUSSION

3.1 Force-Displacement Response

In the force-displacement curve shown in Figure 6 and Figure 7, the experimental results show both force-displacement curves from the left and right directions, respectively. The experimental envelope curves for all wall configurations, derived from each hysteresis loop in the pushing direction ("Experimental (+)") and the pulling direction ("Experimental (-)"), are presented in Figures 6 and 7, respectively. In contrast, the finite ele-



(a) Crack at wall configuration 1 (Triwiyono et al., 2020)

(b) Equivalent Von-Mises stress at FEA model (unit MPa)

(c) Equivalent of total strain at FEA model (Unitless)

(d) Curve of equivalent of total strain and equivalent Von-Mises stress

Figure 9 Failure mode of wall-Configuration 1

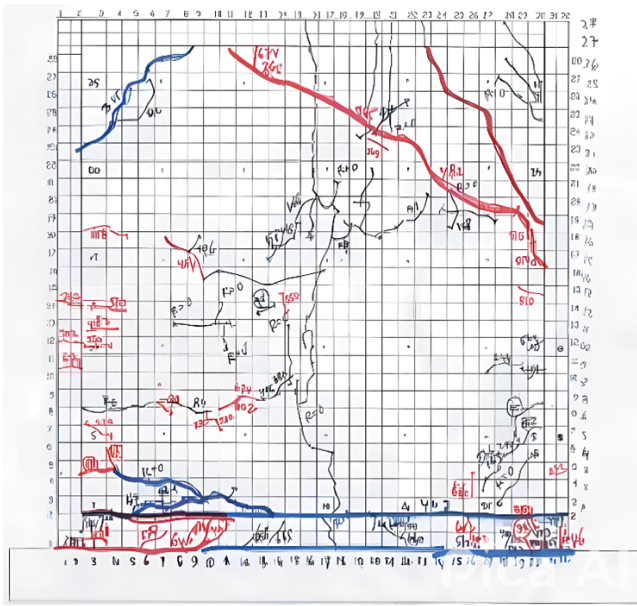
ment analysis (FEA) was conducted under a monotonic static load.

The finite element analysis revealed that the maximum force of brick walls predicted by the finite element model closely aligned with the results from laboratory tests; however, a discrepancy was observed in the initial stiffness values (Triwiyono and Eratodi, 2019). The measured displacements, presented in Figures 6 and 7, were obtained by recording the horizontal displacements at the corners of the wall specimen, which were not subjected to force application in finite element analysis, after being loaded with a maximum force of 7 tons. Figures 6 and 7 show that the elastic displacement-force response of the brick walls is affected by the quality of the concrete forming the column and beam frames.

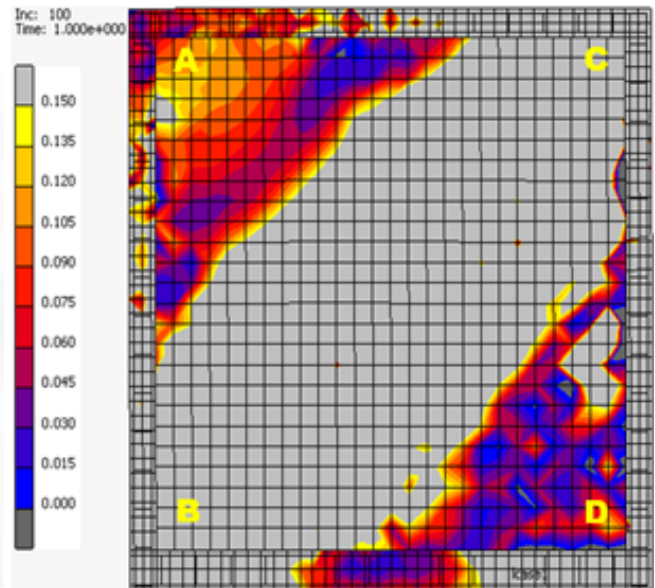
The displacement-force response derived from the finite element analysis conducted in this study demonstrates nonlinear behavior exclusively for Specimen Wall configuration 2, as illustrated in Figure 7. The overall behavior of the brick wall-frame system, as observed in the experimental findings, may still be influenced by the interaction between the brick wall and the surrounding frame.

3.2 Deformed shape of masonry wall

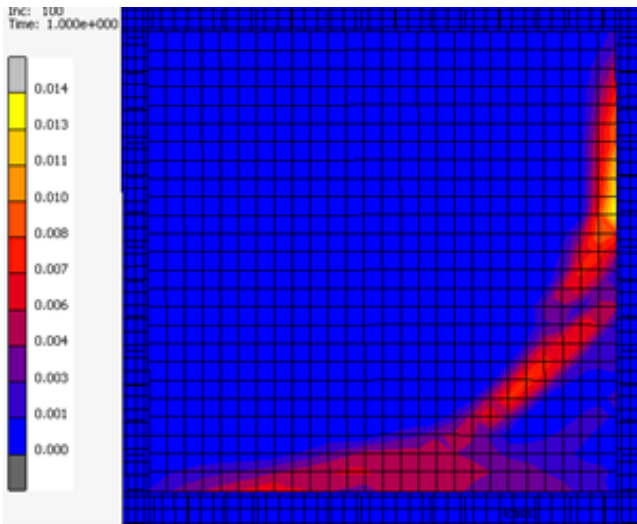
Based on Figures 8a and 8b, experimental observations of both masonry wall configurations 1 and 2 show that there was separation between the tie beam and the foundation, even though steel anchors were installed. The observation also reveals that uplift occurred and



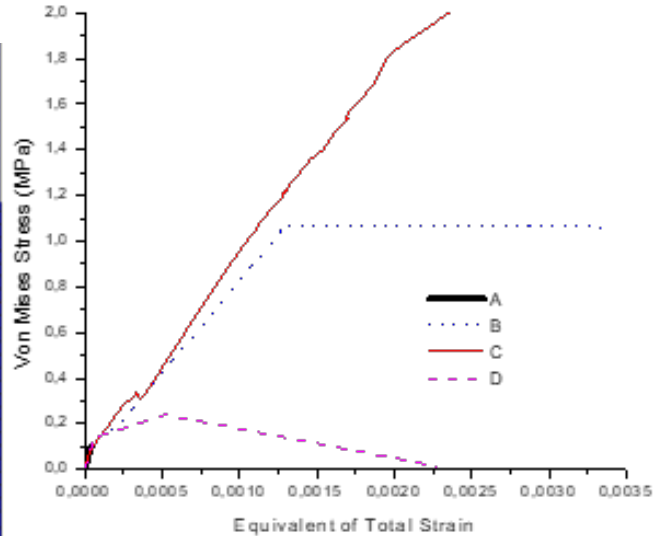
(a) Crack at wall configuration 2 (Triwiyono et al., 2020)



(b) Equivalent Von-Mises stress at FEA model (unit MPa)



(c) Equivalent of total strain at FEA model (Unitless)



(d) Curve of equivalent of total strain and equivalent Von-Mises stress

Figure 10 Failure mode of wall-Configuration 2

spalling was observed at the bottom corner of the concrete frame. The separation between the tie beam and the foundation was deemed inconceivable, despite the installation of steel anchorages (Triwiyono et al., 2020). The results of the finite element analysis do not show any separation, as shown in Figures 8c and 8d. The separation between the tie beam and the foundation did not occur because in the finite analysis modeling, the contact between the tie beam and the foundation was modeled as a Glue contact type where the glue separation was suppressed.

3.3 Failure Modes of Specimen's Reference

The von Mises criteria is among the most commonly used methods for checking yield conditions under multiaxial loading conditions. The von Mises stress can be used as an indicator to determine material failure. In this case, the failure occurs when the equivalent von Mises stress reaches the yield strength of the material in simple tension. The failure mode of the experimental masonry wall for configuration 1 is depicted in Figure 9a. The von Mises stress contours of wall configuration 1 are presented in Figure 9b as well as the crack pattern of the experimental wall shown in Figure 9a. Figure 9b illustrates the maximum von Mises stress, recorded at 0.21 MPa, which corresponds to the tensile strength of the brick masonry. The equivalent

of total strain is often used to predict fracture or permanent deformation. Figure 9c depicts the distribution of equivalent total strain under a 7-ton loading condition, highlighting the strain alignment along the diagonal direction of the wall.

The graph for equivalent von Mises stress versus equivalent total strain at top corner far from loading (point A) of the wall, at top corner near loading finite element analysis (point C) of the wall, and at bottom corner of the wall (point B and point D) can be seen in Figure 9d, respectively. The equivalent von Mises stress at Point A exhibits a linear increase until reaching a maximum value of approximately 0.11 MPa. At Point B, the stress increases linearly up to 0.167 MPa, transitioning to non-linear behavior until it reaches 1 MPa. Similarly, at Point C, the stress remains linear up to 0.243 MPa before exhibiting non-linear behavior, culminating at 1.55 MPa. At Point D, the stress follows a linear trend up to 0.157 MPa, subsequently becoming nonlinear and reaching a maximum value of 0.29 MPa.

Figure 10a illustrates the failure mode of the experimental brick masonry wall for wall configuration 2. The von Mises stress contour for wall configuration 2 is shown in Figure 10b, while the crack pattern of the experimental wall is also presented in Figure 10a. Figure 10b highlights the maximum von Mises stress, measured at 0.15 MPa, which corresponds to the tensile strength of the brick masonry. In contrast to the finite element analysis results for wall configuration 1, where the equivalent of total strain distribution was predominantly diagonal, the total strain contour for wall configuration 2 exhibits a slight inward curvature toward the corners under loading, as depicted in Figure 10c.

In Figure 10d, the equivalent von Mises stress at Point A increases linearly, reaching a maximum value of approximately 0.102 MPa. At Point B, the stress shows a linear increase up to 0.128 MPa, transitions to nonlinear behavior, peaking at 1.07 MPa, and remains constant up to a strain of 0.0033. Similarly, at Point C, the stress increases linearly up to 0.286 MPa before transitioning to nonlinear behavior, ultimately reaching a peak of 2 MPa. At Point D, the stress follows a linear trend up to 0.138 MPa, then transitions to non-linear behavior, and subsequently decreases to 0.01 MPa.

4 CONCLUSION

In this study, three-dimensional finite element analysis was conducted to simulate the nonlinear response of 3D masonry structures using a macro-modeling approach. The brick masonry and concrete were modeled using 3D solid elements with a multi-linear material constitutive model. The compressive failure of brick masonry and concrete was also included via a Linear Mohr-Coulomb material constitutive model. The

tensile strength of brick masonry was taken from experiments, and the tensile strength of concrete was set close to zero to simulate the concrete frame cracking if the von Mises stress exceeded this tensile stress. The steel reinforcement was modeled using 3D truss elements with a bi-linear material constitutive model. The steel and the concrete of the frame were modeled by an embedded model.

The linear force-displacement behavior of brick masonry walls confined by a concrete frame under lateral static forces demonstrates a strong correlation with experimental results. The initial stiffness value derived from finite element analysis exhibits a consistent trend with experimental data. The force-deformation response within the elastic phase is substantiated by nonlinear finite element analysis. However, in the nonlinear phase, the finite element analysis results do not accurately capture the experimental outcomes. Specifically, the analysis yields a linear response for the wall configuration 1 specimens, while the nonlinear response for wall configuration 2 deviates from the experimental results.

The macro-modeling approach used in the finite element analysis for the brick wall elements resulted in differences in the observed damage patterns between wall configuration 1 and wall configuration 2 compared to wall configuration 1 and wall configuration 2 compared to the experimental results. It is recommended that future research include experimental data and numerical studies encompassing a broader range of concrete, brick, and mortar material properties to further generalize the findings and ultimately inform the development of design codes for practical applications.

DISCLAIMER

The authors declare no conflict of interest.

ACKNOWLEDGMENTS

The authors are grateful to the Direktorat Penelitian dan Pengabdian Masyarakat (DPPM), Universitas Islam Indonesia (UII) for providing the research fund. The authors are also grateful for the critical comments of anonymous reviewers and the editor, which helped in improving the quality of this paper.

REFERENCES

- Abdessemed-Foufa, A. (2017), 'Constructive characteristics of the citadel of algiers (algeria)'.
 Arya, A. S., Boen, T. and Ishiyama, Y. (2014), *Guidelines for Earthquake Resistant Non-Engineered Construction*, UNESCO.

- Bhatti, A. Q., Badshah, E., Naseer, A., Ashraf, M., Shah, F. and Akhtar, K. (2017), 'Review of blast loading models, masonry response, and mitigation', *Shock and Vibration* **2017**, 6708341.
- Brzev, S. and Mitra, K. (2007), *Earthquake-Resistant Confined Masonry Construction*, NICEE, National Information Center of Earthquake Engineering, Indian.
- Chaker, A., Rekik, A., Langlet, A. and Hambli, R. (2022), 'Semi-numerical micromechanical model for viscoelastic microcracked masonry', *Mechanics of Materials* **166**, 104218.
- Chen, D., Wu, H. and Fang, Q. (2023), 'Simplified micro-model for brick masonry walls under out-of-plane quasi-static and blast loadings', *International Journal of Impact Engineering* **174**, 104529.
- da Silva, L. C. M. and Milani, G. (2022), 'A fe-based macro-element for the assessment of masonry structures: Linear static, vibration, and non-linear cyclic analyses', *Applied Sciences* **12**(3), 1248.
- Effendi, M. K. (2020), 'Non-linear finite element analysis of flexural reinforced concrete beam using embedded reinforcement modeling', *Journal of the Civil Engineering Forum* **6**(3), 271–284.
- Ewing, B. D. and Kowalsky, M. J. (2004), 'Compressive behavior of unconfined and confined clay brick masonry', *Journal of Structural Engineering* **130**(4), 650–661.
- Gaetano, D., Greco, F., Leonetti, L., Lonetti, P., Pascuzzo, A. and Ronchei, C. (2022), 'An interface-based detailed micro-model for the failure simulation of masonry structures', *Engineering Failure Analysis* **142**, 106753.
- Greco, F., Leonetti, L., Luciano, R., Pascuzzo, A. and Ronchei, C. (2020), 'A detailed micro-model for brick masonry structures based on a diffuse cohesive-frictional interface fracture approach', *Procedia Structural Integrity* **25**, 334–347.
- Grzyb, K. and Jasiński, R. (2022), 'Parameter estimation of a homogeneous macromodel of masonry wall made of autoclaved aerated concrete based on standard tests', *Structures* **38**, 385–401.
- Hendry, A. W. and Khalaf, F. M. (2017), *Masonry Wall Construction*, CRC Press.
- Johansson, P., Wahlgren, P. and Eriksson, P. (2019), Field testing of interior super insulation materials on a brick wall in an industrial building, in 'Proceedings of the 13th International Conference on Thermal Performance of the Exterior Envelope of Whole Buildings', pp. 9–12.
- Marc, M. S. C. (2012a), *Volume A: Theory and User Information*, MSC. Software Corporation.
- Marc, M. S. C. (2012b), *Volume B: Element Library*, MSC. Software Corporation.
- Muhit, I. B., Masia, M. J., Stewart, M. G. and Isfeld, A. C. (2022), 'Spatial variability and stochastic finite element model of unreinforced masonry veneer wall system under out-of-plane loading', *Engineering Structures* **267**, 114674.
- Naciri, K., Aalil, I., Chaaba, A. and Al-Mukhtar, M. (2021), 'Detailed micromodeling and multiscale modeling of masonry under confined shear and compressive loading', *Practice Periodical on Structural Design and Construction* **26**(1), 4020056.
- Noor-E-Khuda, S., Dhanasekar, M. and Thambiratnam, D. P. (2016), 'An explicit finite element modelling method for masonry walls under out-of-plane loading', *Engineering Structures* **113**, 103–120.
- Panto, B., Silva, L., Vasconcelos, G. and Lourenço, P. B. (2019), 'Macro-modelling approach for assessment of out-of-plane behavior of brick masonry infill walls', *Engineering Structures* **181**, 529–549.
- Plassiard, J.-P., Alachek, I. and Plé, O. (2021), 'Damage-based finite-element modelling of in-plane loaded masonry walls repaired with frcm', *Computers & Structures* **254**, 106481.
- Ravichandran, N., Losanno, D. and Parisi, F. (2021), 'Comparative assessment of finite element macro-modelling approaches for seismic analysis of non-engineered masonry constructions', *Bulletin of Earthquake Engineering* **19**, 5565–5607.
- Scacco, J., Ghiassi, B., Milani, G. and Lourenço, P. B. (2020), 'A fast modeling approach for numerical analysis of unreinforced and frcm reinforced masonry walls under out-of-plane loading', *Composites Part B: Engineering* **180**, 107553.
- Triwiyono, A. and Eratodi, I. G. L. B. (2019), Investigation of brick masonry with using of bad quality of bricks and reinforced concrete frame, in 'MATEC Web of Conferences', Vol. 258, p. 04008.
- Triwiyono, A., Eratodi, I. G. L. B., Wibowo, D. E. and Siswosukarto, S. (2020), Investigation of confined masonry using non-standard quality of concrete and reinforcement, in 'International Conference on Sustainable Civil Engineering Structures and Construction Materials', pp. 187–199.
- Weber, M., Thoma, K. and Hofmann, J. (2021), 'Finite element analysis of masonry under a plane stress state', *Engineering Structures* **226**, 111214.
- Öchsner, A. and Öchsner, M. (2016), *The Finite Element Analysis Program MSC Marc/Mentat*, Springer.

[This page is intentionally left blank]